Validating, documenting and qualifying models used for consequence assessment of hydrogen explosion scenarios

Helene Hisken [a,b], Gordon Atanga [a], Trygve Skjold [a], Sunil Lakshmipathy [a] & Prankul Middha [a]

E-mail: Helene.Hisken@gexcon.com

[a] Gexcon AS, Bergen, Norway
[b] University of Bergen, Department of Physics and Technology, Bergen, Norway

Abstract

This paper explores a systematic methodology for validating, documenting and qualifying models used for consequence assessment of accidental explosion scenarios. To demonstrate the advantages of implementing and maintaining an integrated framework, example validation cases relevant for the modelling of vented hydrogen deflagrations are presented. Simulations were performed using the computational fluid dynamics (CFD) tool FLACS-Hydrogen. The main focus of this study is on the definition and application of a model evaluation protocol (MEP), building on recent advances from the hydrogen safety community. Particular emphasis is put on the classification of experiments in the validation database. The present methodology is found to be highly useful for qualifying a model system for specific applications as well as for highlighting areas where further development is needed.

Keywords: *model evaluation protocol, CFD modelling, hydrogen safety, vented explosions*

1. Introduction

Fires and explosions represent a significant hazard for hydrogen installations, such as electrolysers, fuel cell backup systems and refuelling stations, and special measures must be applied to reduce the risk to an acceptable level (Skjold *et al.*, 2015). For example, the accidental release and ignition of hydrogen from high-pressure systems located in containers – such as those found at hydrogen refuelling stations – may lead to violent explosions (Sommersel *et al.*, 2015). Installing pressure relief panels can provide effective mitigation against the consequences of gas explosions in these enclosures.

Quantitative risk assessment (QRA) is an important tool for managing the risk associated with hydrogen systems, and for developing and revising hydrogen regulations, codes and standards. It is crucial that the models, data and assumptions underlying the QRA are valid. Groth & Hecht (2015) emphasise that consequence models used in QRA studies should be extensively validated against experiments relevant for their application range. Systematic verification and validation is also essential for quality assurance: continuously monitoring the effects of changes in source code, compilers or operating systems.

The objective of the present paper is to investigate how the validation methodology proposed by Skjold *et al.* (2013) can be applied to models used for consequence assessment of accidental hydrogen explosion scenarios. The model evaluation protocol (MEP) described in the present paper is based on work by the Model Evaluation Group (MEG) and the Model Evaluation Group for Gas Explosions (MEGGE) set-up by the European Union (MEG, 1994ab; MEGGE, 1996). Ivings *et al.* (2007; 2013) presented a protocol for the evaluation of LNG vapour dispersion models, including a set of statistical performance measures (SPM) for quantitative assessment of model performance similar to those proposed by Hanna *et al.* (1991ab; 1993). The present MEP applies several of these principles. Finally, the MEP builds on the important work performed as part of the SUpport to SAfety aNAlysis of Hydrogen and Fuel Cell Technologies (SUSANA) project (co-funded by the Fuel Cell and Hydrogen JU, 2013-2016), described by Baraldi *et al.* (2015). Baraldi *et al.* (2015) presented the model evaluation protocol HyMEP,

developed specifically for computational fluid dynamics (CFD) models. The validation database for HyMEP is organised according to the physical phenomena involved in the experiment (i.e. release and dispersion, ignition, deflagration, deflagration-to-detonation transition (DDT), and detonations), and includes an extensive suite of verification tests.

Skjold *et al.* (2013) described the components of an integrated framework for validating model systems: (i) a validation database, (ii) a model evaluation protocol, (iii) a model system, and (iv) a set of standardised procedures for documenting model performance in reports, manuals and training material. In this framework, the MEP defines the overall structure of the validation database by employing criteria for classifying and prioritising validation cases based on parameters such as relevance for typical applications of the model system, availability of data, etc., in addition to criteria for evaluating model performance. The methodology also includes tools for setting up, running, and processing model results, and documented file formats for storing data from experiments and simulations.

The present validation methodology mainly differs from the work described by Baraldi *et al.* (2015) through its approach for classifying and prioritising the experiments in the validation database. Furthermore, the paper focuses on demonstrating how a MEP can be applied specifically for consequence assessment of accidental deflagration scenarios involving hydrogen mixtures in small-scale enclosures or 20 ft. or 40 ft. ISO containers, relevant e.g. for QRA studies of hydrogen refuelling stations. The present MEP should in principle be applicable to any type of consequence model (analytical model, empirical correlation, CFD model, etc.). In this paper, the CFD tool FLACS-Hydrogen (Gexcon, 2015) is used for selected example validation cases to demonstrate the approach.

The MEP proposed by Skjold *et al.* (2013) essentially follows the six-step evaluation procedure proposed by MEGGE (1996): 1) validation database description, 2) model description, 3) scientific assessment, 4) verification, 5) user-oriented assessment, and 6) model validation. In the following, Section 2 presents the overall validation database structure, and outlines the approach for classifying experiments. Section 3 summarises the required content of the model description, the scientific assessment and model verification. Validation and model performance criteria are discussed in Section 4. Assessment of the user experience is not further discussed in the present paper.

2. Database description

The validation database may contain many types of instances: experimental campaigns, real accidents and analytical solutions (verification tests). The validation methodology presented by Skjold *et al.* (2013) focuses on identifying the key physical phenomena in the validation experiments, and assessing how the model represents each of these phenomena. Hence, for gaseous deflagrations, the organisation of validation data is primarily according to the *degree of congestion* and the *degree of confinement* in the experiments, as illustrated by Fig. 1.

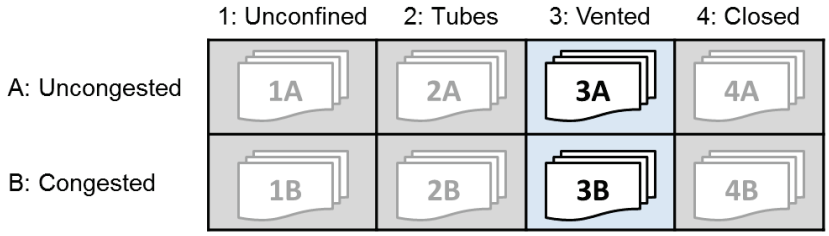

Fig. 1 *Classification of gas explosion validation cases (Skjold et al., 2013). Categories 3A and 3B are relevant for the present study.*

As the validation database used in the present study only includes instances relevant for explosion scenarios involving hydrogen mixtures in vented small-scale enclosures or 20 ft./40 ft. ISO containers, the present validation database is limited to the categories "3A: empty vented enclosures" and "3B: vented enclosures with obstacles" in Fig. 1. Table 1 provides examples of relevant instances for the present application. Within each application area and sub-category, the classification of validation experiments considers five parameters: relevance and context, spatial scale, repeatability, measurement quality, and the availability of data.

***Table 1**: Examples of relevant instances in the validation database. The database is extended and updated as additional experiments are identified or new information becomes available.*

Subcategory	Description	Reference
Empty vented enclosures/vented enclosures with obstacles	Hydrogen-air deflagrations performed in a 64 m^3 vented explosion chamber.	**Exp./Sim.**: Bauwens *et al.* (2011), Chao *et al.* (2011), Bauwens *et al.* (2012), Bauwens & Dorofeev (2014) **Sim.**: Jallais & Kudriakov (2013), Keenan *et al.* (2014), Vyazmina & Jallais (2015)
	Hydrogen-air deflagrations performed in a 1 m^3 vented explosion chamber.	**Exp.**: Kuznetsov *et al.* (2015) **Sim.**: Baraldi *et al.* (2015), Vyazmina & Jallais (2015)
	Deflagration experiments involving inhomogeneous hydrogen-air clouds generated by realistic releases in a standard 20 ft. ISO container (≈ 40 m^3).	**Exp.**: Sommersel *et al.* (2015) **Exp./Sim.**: Sommersel *et al.* (2008)
	Hydrogen-air deflagrations performed in a 25 m^3 vented explosion chamber.	**Exp./Sim.**: Marangon *et al.* (2009), Schiavetti & Carcassi (2013)
	Hydrogen-air deflagrations performed in a 0.68 m^3 vented explosion chamber.	**Exp./Sim.**: Schiavetti & Carcassi (2013)
	Hydrogen-air deflagrations performed in a 4 m^3 vented explosion chamber.	**Exp.**: Daubech *et al.* (2013) **Sim.**: Jallais & Kudriakov (2013), Vyazmina & Jallais (2015)
Empty vented enclosures	Hydrogen-air deflagration experiments performed in a 120 m^3 vented explosion chamber.	**Exp.**: Kumar (2006) **Sim.**: Makarov & Molkov (2013), Jallais & Kudriakov (2013)
	Hydrogen-air deflagration experiments performed in a 0.95 m^3 cylindrical vented explosion chamber.	**Exp.**: Pasman *et al.* (1974) **Sim.**: Baraldi *et al.* (2010), Jallais & Kudriakov (2013), Vyazmina & Jallais (2015)
	Hydrogen-air deflagrations experiments performed in a 1 m^3 cylindrical vented explosion chamber.	**Exp.**: Daubech *et al.* (2011) **Sim.**: Jallais & Kudriakov (2013), Vyazmina & Jallais (2015)
	Hydrogen-air deflagrations experiments performed in a 10.5 m^3 cylindrical vented explosion chamber.	**Exp.**: Daubech *et al.* (2011) **Sim.**: Jallais & Kudriakov (2013), Vyazmina & Jallais (2015)

2.1 Validation example: FM Global 64 m^3 vented chamber

A series of publications describe experimental campaigns conducted in the vented explosion chamber of dimensions 4.6 m × 4.6 m × 3.0 m located at the FM Global research campus, highlighting the physical phenomena that produce separate, distinct pressure peaks in vented gas explosions. The effects on peak overpressures of varying the vent size (either 5.4 m^2 or 2.7 m^2), the ignition position ("back", "central" or "front" with respect to the vent opening), the initial turbulence level, and the fuel concentration of hydrogen-air mixtures are presented in (Bauwens *et al.*, 2011; Chao *et al.*, 2011; Bauwens *et al.*, 2012; Bauwens & Dorofeev, 2014).

In addition, several of the experimental campaigns investigate the effect of inserting eight square obstacles of dimensions 0.4 m × 0.4 m, spanning the vertical direction of the explosion chamber.

2.1.1 Classification

The tests performed without obstructions are relevant for validation category 3A "empty, vented enclosures", while the experiments with obstructions are associated with category 3B "vented enclosures with obstacles" in Fig. 1. The present study is limited to the experiments performed in empty enclosures.

2.1.2 Description of physical phenomena

Bauwens *et al.* (2011) investigated Lewis number effects in the quasi-laminar and turbulent phase of flame propagation for lean hydrogen mixtures (18 ± 0.5 vol % hydrogen in air) by comparing with results for methane and propane-air mixtures with similar laminar burning velocities. For fuel-lean hydrogen-air mixtures, thermal-diffusive effects significantly enhance the flame surface area wrinkling due to the Darrieus-Landau instability (Darrieus, 1938; Landau, 1944). Furthermore, the dependency of the turbulent burning velocity on the turbulence velocity fluctuation u' changes with a varying Lewis number, or more rigorously, a varying Markstein number (see e.g. Bradley *et al.*, 2005). These effects were also explored by Bauwens *et al.* (2012), presenting results for lean hydrogen-air mixtures with varying fuel concentrations (thus effectively varying the Lewis or Markstein number of the mixture). Bauwens & Dorofeev (2014) presented results for experiments where both the initial turbulence levels and hydrogen concentrations varied systematically.

Overall, the pressure-time histories for tests in the empty enclosures exhibit two distinct pressure peaks. The first pressure peak, denoted as P_{ext}, is generated by the external explosion. Prior to flame arrival at the vent, unburnt mixture is pushed out of the vent opening, in particular for back and centre ignition. When the flame front reaches the vent opening, the external turbulent fuel-air cloud ignites. The Rayleigh-Taylor instability, occurring when a less dense fluid accelerates into a denser fluid, may increase the flame surface area and promote the mass combustion rate as the flame front exits the chamber. The overpressure generation by the external explosion reduces the rate of venting from the chamber; the external explosion may or may not be in phase with the Helmholtz oscillations through the vent opening, initiated by the venting of combustion products. In the oscillation phase, the Rayleigh-Taylor instability will again be triggered on the flame surface, further promoting the combustion rate when the density gradient is accelerated in the unstable direction. For the presently investigated experimental campaigns, variations in P_{ext} up to ± 25 % between repeated tests were reported (Chao *et al.*, 2011).

Flame-acoustic interactions were found to generate the second pressure peak, denoted as P_{vib}. Two distinct types of acoustics were identified in the present campaigns: i) low-frequency oscillations matching the first fundamental mode of a wave propagating inside the chamber parallel to the vent opening, assuming the chamber is filled with combustion products (~100 Hz) and ii) high-frequency vibrations corresponding to the natural frequency of various structural components of the chamber (~700 Hz) (Bauwens *et al.*, 2009). P_{vib} particularly dominates for front-ignition, due to the higher amount of unburned gas and larger flame surface area present in the chamber at the time that acoustics develop, when compared to tests with back and centre ignition. P_{vib} is important for empty vented enclosures, as the presence of

obstacles dampen flame-acoustics interactions. Chao *et al.* (2011) reported variations in P_{vib} of ± 50 % between repeated tests.

2.1.3 Prioritisation

In the following, the experimental campaigns presented by Bauwens *et al.* (2011; 2012) and Bauwens & Dorofeev (2014) are evaluated with respect to their relevance for safety studies of installations where hydrogen systems are enclosed in 20 ft. ISO containers. The evaluation applies the assessment criteria listed in Section 2.

Relevance and context

The most important criterion with respect to prioritising validation cases is the application area for the model system, and to what extent the physical phenomena encountered in an experiment are representative for the events that should be simulated. Table 2 summarises the range of scores that can be assigned to an instance for *relevance and context*.

As described in Section 2.1.2, the experiments presented by Bauwens *et al.* (2011; 2012) and Bauwens & Dorofeev (2014) systematically investigate the physical phenomena producing the pressure peaks in empty vented enclosures with fuel-lean hydrogen-air mixtures. Enclosures with obstacles may have higher relevance for the final application of the model system, however, several of the physical processes analysed for the empty vented enclosures will also be important when obstacles are present. The lean hydrogen-air mixtures are clearly relevant for practical hydrogen applications.

***Table 2**: Categories for the relevance and context of the experiments.*

Scale	Description
3: Highly relevant	The experiments involve phenomena that are highly relevant for industrial practice
2: Quite relevant	The experiments involve phenomena that are quite relevant for industrial practice
1: Somewhat relevant	The experiments involve phenomena that are somewhat relevant for industrial practice
0: Not relevant	The experiments are only remotely relevant for industrial practice

Spatial scale

Phenomena that govern the results obtained in small-scale laboratory experiments may not be equally important in large scale, and vice versa. Note that the scores related to the *spatial scale* of the experiments listed in Table 3 are relative to the spatial scale of the final application.

Typical "full-scale" experiments for the 20 ft. ISO container application will entail volumes of flammable gas exceeding 40 m^3. The present experimental enclosure is 64 m^3, and is therefore classified in the validation database as a "full-scale" experimental rig.

***Table 3**: Categories for the spatial scale of the experiments.*

Scale	Description
3: Full-scale	Experiments representative of actual (full-scale) industrial applications
2: Medium-scale	Experiments downscaled by a factor 1.5-5 of actual industrial applications
1: Small-scale	Experiments downscaled by a factor > 5 of actual industrial applications
0: Lab-scale	Results from 20-litre vessels, burners and other experiments at laboratory scale

Repeatability

Table 4 summarises the relevant categories for the *repeatability* of a validation experiment. Experiments that show good repeatability is likely to be controlled by known input parameters, and hence more likely to be reproduced by a proper model. Repeatability should ideally characterise the physical phenomena rather than the measurement quality.

For the present validation examples, Chao *et al.* (2011) reported the variations in P_{ext} and P_{vib} between repeated tests separately. In particular, the phenomena governing P_{vib} are inherently highly variable, ± 50 % between repeated tests. The effects of varying selected input parameters,

i.e. the initial fuel concentration and the initial turbulence velocity, are systematically investigated in the experiments and therefore well known. The repeatability is therefore considered to be above "acceptable", corresponding to a score of 2.5 (cf. Fig. 2a).

***Table 4**: Categories for the repeatability of experiments.*

Scale	Description
3: Excellent	Most of the experiments have been repeated and the repeatability is good
2: Acceptable	Some of the experiments have been repeated, with reasonable repeatability
1: Unknown	None of the experiments/instances have been repeated (e.g. accidents)
0: Poor	Some of the experiments have been repeated, but with very poor repeatability

Measurement quality

It is essential to know the characteristics of the measurement system, and whether and how the original data have been processed: filter specifications, averaging techniques, correction of data to account for instrument errors, etc. It is also important to evaluate whether the relevant parameters were measured, as well as the density of the measurements. Table 5 summarises the categories for *measurement quality,* with examples relevant for gas explosion experiments.

In the present validation case, the measurement systems and techniques are characterised; error bars are given e.g. for concentration measurements. Several pressure-time and flame velocity curves are presented, the degree of filtering and other techniques for post-processing are well-defined, and the systems have been used and described for a range of experimental campaigns in several publications. The measurement quality is therefore assumed to be "excellent".

***Table 5**: Categories for the quality of the measurements.*

Scale	Description
3: Excellent	Reliable measurements of several relevant variables: pressure, flame arrival times, etc.
2: Moderate	Reliable measurements of at least one variable (e.g. pressure-time histories)
1: Poor	Only measurements of questionable quality available
0: Absent	No relevant measurements available

Availability of data

Table 6 summarises the classification of experimental data with respect to *availability*. Sufficient access to information about the validation instance is crucial. However, it may still be worthwhile to simulate experiments or accidents for which limited data are available, as long as sufficient caution is exercised during the model evaluation.

According to Table 6, the availability of data for the present validation examples are classified as "moderate". The magnitudes of P_{ext} and P_{vib} are listed for all the experimental configurations, while pressure-time and flame velocity curves are presented for selected configurations.

***Table 6**: Categories for the availability of experimental data.*

Scale	Description
3: Excellent	All necessary information available: reports, raw data, processed data, videos, etc.
2: Moderate	Most relevant information available: reports, publications, etc.
1: Poor	Significant information missing: only point measurements available
0: None	No quantitative information available

Overall priority

The categorisation defined by Table 2 - Table 6 may be used to prioritise the experimental campaigns for validation, and to determine which experimental campaigns should be emphasised in the model evaluation. Fig. 2 shows radar plots summarising the categorisation for the three first instances in Table 1, relative to the 20 ft. ISO container application. Note that any low scores here mainly are associated with lack of data, and that the experiment evaluation

would change when various applications are considered, or as new information becomes available.

The hydrogen-air explosion tests performed in an empty 64 m^3 vented chamber, presented by Bauwens *et al.* (2011; 2012) and Bauwens & Dorofeev (2014), are considered to be of high quality, and relevant for the final application. The availability of results is sufficient to recommend that the experiments should be modelled. The assigned scores are visualised in Fig. 2a.

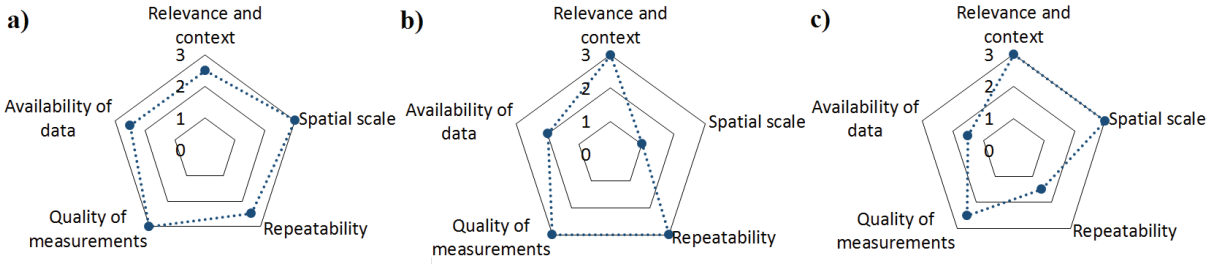

Fig. 2 *Radar plots of three instances in Table 1, a) FM Global 64 m^3 chamber b) KIT 1 m^3 c) Telemark ISO container.*

3. Model characterisation

The *model description* should (at least) include the following information: 1) name and version number, 2) application area, 3) model type, 4) the institution where the tool has been developed, 5) formal requirements for use, and 6) a list of relevant references. Following MEGGE (1996), the model evaluation should also include a comprehensive description of the model system, together with an *assessment of the scientific content*. Limits of model applicability and advantages should be explained, together with suggestions for possible improvements.

Model verification is the process of asserting that the implementation produces output in accordance with the given specifications, and is normally an integrated part of model development. Appropriate verification tests for each model system are defined as separate instances in the validation database. Model verification is crucial; however, defining and performing verification exercises is outside the scope of the present paper.

3.1 Validation example: the CFD tool FLACS-Hydrogen

This section briefly summarises and discusses selected components of the numerical solver in FLACS-Hydrogen, version 10.4, release 2 that are relevant for the present validation example. FLACS-Hydrogen is used for consequence assessment of accidental release and explosion scenarios for a wide range of industrial applications. The CFD tool is developed by Gexcon (2015), and requires a commercial or academic licence.

FLACS-Hydrogen solves the three-dimensional Favre-averaged conservation equations for mass, momentum, enthalpy h, mass-fraction of fuel Y_f, mixture-fraction ξ, turbulent kinetic energy k, and rate of dissipation of turbulent kinetic energy ε on a structured Cartesian grid. The standard k-ε model (Launder & Spalding, 1974) is used to represent turbulence, and the equations are closed by invoking the ideal gas equation of state. Boundary layers are not resolved, instead wall-functions are used to compute turbulence production and drag forces for objects that are on-grid, i.e. larger than the size of a computational cell. Geometry is represented on the computational grid using the porosity/distributed resistance (PDR) concept (Patankar & Spalding, 1974; Sha & Launder, 1979; Sha *et al.*, 1982; Hjertager, 1986). A volume porosity β_v, denoting the ratio of open volume to the total volume of each computational cell, is computed prior to the simulation. Similarly, the area porosity β_j is defined as the ratio of the projected open area between two neighbouring cell centres to the total area of the respective control volume face in the jth direction. In the following, β_j is excluded from the Einstein

summation convention in the partial differential equations. Using the finite volume approach, the conservation equation for the general variable Φ (representing either 1, u_i, h, k, ε, Y_f or ξ) is integrated over the porous part of the control volume. The general equation on integral form reads

$$\int_{V_{CV}} \frac{\partial}{\partial t}\left(\beta_v \rho \Phi\right) dV + \int_{A_{CV}} n_j \left(\beta_j \rho \Phi u_j\right) dA = \int_{A_{CV}} n_j \left(\beta_j \Gamma_\Phi \frac{\partial \Phi}{\partial x_j}\right) dA + \int_{V_{CV}} \beta_v \left(S_\Phi + R_\Phi\right) dV \,, \tag{1}$$

where ρ is the fluid density, u_j is the fluid velocity in the jth direction, n_j is the vector normal to the control volume surface pointing outwards in the jth direction, Γ_Φ is the effective turbulence diffusion coefficient, S_Φ is the source term for Φ, and R_Φ represents additional resistance, additional mixing and/or additional heat transfer caused by solid obstructions in the flow. Sub-grid models are applied to represent the terms S_Φ and R_Φ in Equation (1). The code uses a 2nd-order central differencing scheme for diffusive fluxes and a 2nd-order hybrid scheme with weighting between upwind and central difference (with delimiters for some equations), for convective fluxes. Time-marching is carried out using the 1st-order implicit backward Euler scheme and the discretized equations are solved using the BICGStab iterative method with the SIMPLE pressure correction algorithm.

An extensive, thorough discussion on the applicability of RANS modelling for simulating industrial-scale gas explosions is outside the scope of this paper. In the following, a few relevant model components are described to support the analysis of the model performance in Section 4.1. More complete descriptions of the model system and its limits of applicability are available in e.g. (Gexcon, 2015; Arntzen, 1998; Middha, 2010).

3.1.1 Relevant sub-grid models and possible limitations

Premixed combustion in FLACS-Hydrogen is modelled by the conservation equation for the fuel mass fraction Y_F according to

$$\frac{\partial}{\partial t}\left(\beta_v \rho\, Y_F\right) + \frac{\partial}{\partial x_j}\left(\beta_j \rho Y_F u_j\right) = \frac{\partial}{\partial x_j}\left(\beta_j \Gamma_{Y_F} \frac{\partial Y_F}{\partial x_j}\right) + w_F \,. \tag{2}$$

The sink term w_F in Equation (2) represents the Favre-averaged consumption rate of reactants, producing combustion products by chemical reaction. The reaction rate w_F and the effective diffusion coefficient Γ_{YF} are modelled such that the numerical flame zone propagates with a certain input burning velocity (Arntzen, 1998). Empirical correlations relating the burning velocity to the flow regime and mixture dependent variables are needed to close Equation (2). Burning velocity correlations are therefore defined for *laminar*, *quasi-laminar* and *turbulent* flow conditions.

The burning velocity in all flow regimes incorporates the laminar burning velocity u_l, which can be regarded as a fundamental property of the mixture, representing its reactivity, diffusivity and exothermicity (Ranzi *et al.*, 2012). FLACS-Hydrogen uses a library of literature laminar burning velocities to represent u_l. For an initially laminar, outwardly propagating flame, hydrodynamic (Darrieus, 1938; Landau, 1944) and thermo-diffusive flame instabilities (Barenblatt *et al.*, 1962; Sivashinsky, 1977) will lead to the appearance of a cellular flame surface at a critical flame radius $R_{f,cr}$. The transition into a cellular regime of flame propagation is associated with an increase in flame surface area and a corresponding increase in the overall burning velocity. To model the regime of cellular flame propagation, a so-called quasi-laminar burning velocity u_{ql} on the form of

$$u_{ql} = u_l \left(1 + C_{ql} R_f^a\right), \tag{3}$$

where C_{ql} is a mixture-dependent model constant, R_f is the flame radius and a = 0.5 (based on gas explosion experiments performed at CMI as part of the Gas Safety Programme (GSP) 90-92), is applied in FLACS-Hydrogen.

A range of expressions relating turbulence variables to the combustion rate in turbulent premixed flames have been proposed. Based on the 1650 separate measurements of turbulent burning velocities for premixed gaseous mixtures consolidated by Abdel-Gayed *et al.* (1987), Bray (1990) expressed the turbulent burning velocity u_t in terms of the Karlovitz stretch factor K according to

$$\frac{u_t}{u'} = \alpha K^{\beta}, \tag{4}$$

where $K = C_K\,(u'/u_l)^2(u'\ell_I/\nu)^{-0.5}$, $C_K = 0.157$, u' is the turbulence velocity fluctuation, ν is the kinematic viscosity, and ℓ_I is the integral length scale of turbulence. The turbulent burning velocity correlation in FLACS v10.4r2 (Gexcon, 2015) is given by Equation (4), where α = 0.875 and β = -0.393.

Fuel-lean hydrogen-air mixtures (with a hydrogen concentration less than ≈ 20 %) are characterised by negative Markstein numbers at atmospheric pressure; such mixtures exhibit higher burning rates when exposed to positive stretch rates, are less likely to quench at high stretch rates, and are more prone to develop flame instabilities than mixtures with positive Markstein numbers. In FLACS-Hydrogen, a Lewis number dependent correction is applied directly to the laminar burning velocity, to account for thermo-diffusive effects in both the quasi-laminar and turbulent regime of flame propagation. However, Lewis or Markstein number effects may have a different influence on the burning rate for different combustion regimes. Consequently, this sub-model may be a source of inaccuracy for simulating fuel-lean hydrogen-air deflagrations. Recently, Bradley *et al.* (2013) published a correlation where α and β are expressed explicitly in terms of the mixture's stretch rate Markstein number. Applying a Markstein number dependent burning velocity correlation would strictly be more general than applying fixed values for α and β in Equation (4) for any mixture.

Increase in flame surface area due to the Rayleigh-Taylor instability is currently not modelled in FLACS v10.4r2, therefore, the external explosion is represented by turbulence production by flow through the vent opening alone. Furthermore, FLACS-Hydrogen currently does not have sub-grid models accounting for flame surface area enhancement due to acoustics-flame interactions. Section 4.1.6 includes further discussion on the limits of applicability of the model system in light of selected validation results.

4. Validation

Validation against experiments is the process of showing that a model reproduces measurements of specific physical parameters to satisfactory accuracy within its stated range of applicability (Ivings *et al.*, 2013). The validation procedure of the present MEP includes 1) description of primary and secondary target variables for validation, 2) selection of instances from the validation database, 3) description of model input and assumptions for each validation case, 4) sensitivity studies, 5) qualitative assessment of model performance, 6) quantitative assessment of model performance through appropriate statistical performance measures (SPM), and 7) overall assessment of model performance and communication to the user.

Variables that are directly relevant for the intended use of the model should be weighted more heavily than those of peripheral interest (MEGGE, 1996). In the present MEP, used for vented hydrogen deflagrations, variables representing the magnitude of the explosion overpressure are listed as primary validation targets, while other variables are assumed to be of secondary importance. For example, the maximum obtained (gauge) overpressure inside the vented

enclosure, denoted P_{max} (for many correlations, the denotation P_{red} is used), is a primary target, while (if applicable) the time of occurrence of the maximum overpressure (measured after ignition) in a specific location with coordinates (x,y,z) is a secondary target. If possible, distinct pressure peaks, such as P_{ext} and P_{vib}, should be considered separately. The selection of experiments from the validation database used for model evaluation can be made based on the criteria described in Section 2.

Model input and assumptions must be documented for each validation instance, so that the results can be easily reproduced. The sensitivity of the relevant validation targets to the initial conditions, such as mixture properties and initial turbulence levels, etc. must be evaluated. Furthermore, if applicable, the sensitivity of the relevant results to applying different boundary conditions and simulation domain sizes should be explored. Whenever applicable, the sensitivity of validation targets to the degree of resolution in time and space must be assessed. If grid convergence cannot be obtained, at least two different grid resolutions should be investigated, and differences in the relevant validation targets must be reported.

For the present application of hydrogen deflagrations, detailed plots of the pressure-time development and the flame speed vs. distance should be produced and compared to experimental measurements whenever possible. The *qualitative assessment* of a model's performance addresses whether the relevant trends in the validation variables with changes in experimental parameters are reproduced. To perform *quantitative assessment* of the model performance, a set of statistical performance measures (SPM) are defined. According to Duijm & Carissimo (2002), SPM should provide (i) a measure of bias in model predictions, i.e. the tendency of a model to systematically over-or under-predict relevant variables, and (ii) a measure of the spread in predictions, i.e. the degree of scatter around a mean value. The statistical evaluation of a validation study may utilise parameters such as those defined by Hanna *et al.* (1991ab; 1993) and Ivings *et al.* (2007). In Table 7, X_P is the predicted value of a relevant variable in a validation case, X_O is the observed value, and the operator < > is the arithmetic mean. The fractional bias (FB) and geometric mean bias (MG) represent the bias in model predictions, while the normalised mean square error (NMSE) and the geometric mean variance (VG) represent the scatter in the model predictions around a mean value. Hanna *et al.* (1993) recommend that all SPM from Table 7 be used together for the quantitative assessment.

***Table** 7: Parameters for statistical evaluation of validation results.*

Name	Definition
Fractional bias (FB)	$(\langle X_P \rangle - \langle X_O \rangle) / 0.5(\langle X_P \rangle + \langle X_O \rangle)$
Normalised mean square error (NMSE)	$\langle (X_P - X_O)^2 \rangle / \langle X_P \rangle \langle X_O \rangle$
Fraction within a factor of two (FAC2)	Fraction of the data that satisfies $0.5 \le X_P / X_O \le 2$
Geometric mean bias (MG)	$\exp(\langle \ln\{X_P / X_O\} \rangle)$
Geometric mean variance (VG)	$\exp(\langle (\ln\{X_P / X_O\})^2 \rangle)$

The assessment of model performance should be summarised for each target variable, for each experimental series. Experience is needed in order to define appropriate criteria for a "good" model (Ivings *et al.,* 2013), so the assessment criteria for the validation targets should be updated as the MEP is used. In general, when a consequence model is used for safety applications, a moderate over-prediction, such as a MG of 1.3, will be preferred over a moderate bias for under-prediction, such as a MG of 0.77. Here, "excellent" model performance in terms of the validation target P_{max} from an experimental campaign is characterised by the measured variable being reproduced with a 0.77 < MG < 1.3 (i.e. a mean bias within a factor of 1.3), and a VG < 1.6 ("factor two scatter"). Furthermore, the measured variable should be reproduced

with a FAC2 of 75 %, and key trends in the prediction of the measured variable should be consistent with the experiments. For "acceptable" model performance, the measured P_{max} should be reproduced within 0.5 < MG < 2 (i.e. a mean bias within a factor of two), VG < 3.3 ("factor three scatter") and FAC2 of 50 %. Requirements for NMSE and FB are not yet defined, and will be added as further experience is gained. Ideally, experimental variability should also be taken into account in the model evaluation.

The results from the model evaluation process should be summarised as a set of user guidelines/recommendations, defining the domain of applicability of the model system. The SPM for appropriate groups of experimental campaigns should be communicated. If confidential experimental results are used for validation, the SPM can be restricted to normalised results, e.g. MG and VG as defined in Table 7. Section 4.1.5 demonstrates how SPM can be visualised.

4.1 Validation example: FM Global 64 m³ vented chamber

The present section evaluates model performance for the example validation case from Section 2.1. Simulations were performed using the standard FLACS-Hydrogen release, version 10.4r2 (denoted FLACS v10.4r2), described in Section 3. Following the MEP, sections 4.1.2 and 4.1.3 present sensitivity studies for the model system. Section 4.1.4 discusses model representation of the physical phenomena; Section 4.1.5 presents selected statistical parameters for model evaluation, while Section 4.1.6 summarises the results, and suggests possible model improvements.

4.1.1 General remarks to the simulation setup

The simulation domain was set to 40 m × 30 m × 12 m, to allow for sufficient distance to the boundaries. The geometry of the experimental rig and the ignition points were defined according to the information in the available publications.

4.1.2 Sensitivity of results to grid resolution

Simulations were performed using grid resolutions of 0.20 m, 0.10 m or 0.05 m inside the chamber. The same grid refinement was used up to 4 m outside the vent opening to capture the external explosion, while a coarser (stretched) grid was applied outside the core domain. Fig. 3 (left) shows the maximum observed grid dependency of the peak overpressure (60 % higher overpressure for a grid resolution of 0.2 m compared to a grid resolution of 0.05 m), centre ignition, with a 5.4 m² vent opening. Similar grid dependency was found for centre ignition, with a 2.7 m² vent opening, while the other configurations showed variations of less than 20 % with each refinement.

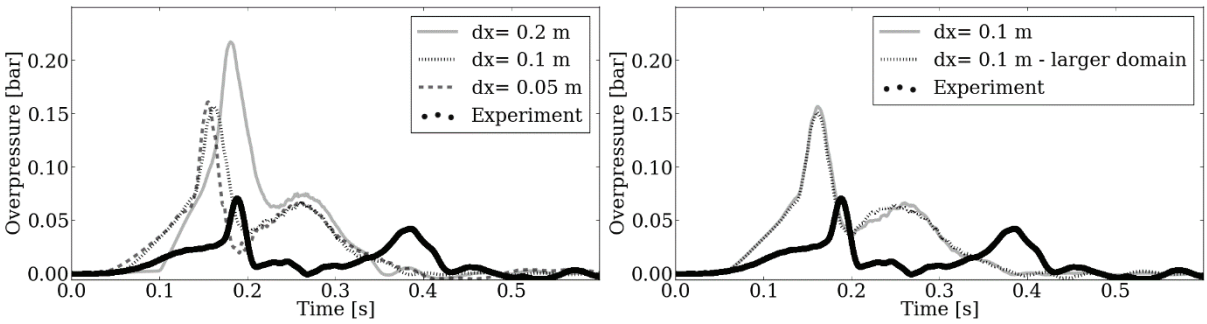

Fig. 3 *Grid sensitivity (left), and sensitivity to size of simulation domain (right), centre ignition, 5.4 m² vent, pressure-time.*

The main features of the pressure-time curves were similar for all grid resolutions; however, the 0.10 m and 0.05 m grid sizes generally resulted in less over-prediction than for 0.20 m. The simulations in the following sections applied a grid resolution of 0.10 m.

4.1.3 Sensitivity of results to initial and boundary conditions

The maximum overpressures vary with < 1 % for perturbations in the initial turbulence velocity u' of ± 0.01 m/s. The sensitivity to the hydrogen concentration is significant around the reference concentration of 18 % hydrogen in air (used for all tests in Bauwens *et al.*, 2011) – maximum simulated overpressures vary with ± 25 % over the experimental uncertainty range of ± 0.5 %. The effects of varying the initial fuel concentration were consistent with results from a dedicated test series (Bauwens *et al.*, 2012). The results are relatively insensitive to variations in initial temperature of ± 5 ºC; maximum overpressures varied with < 5 %.

The initial value for the turbulence length scale in the simulations determines the initial conditions for the dissipation rate ε in the k-ε model. The representation of the external explosion appears to be particularly sensitive to the initial conditions for ε; a change in the turbulence length scale from 10 % to 20 % of the grid cell size gives an increase in maximum overpressures of 40 %. In the following analysis, the initial length scale is set to 10 % of the grid cell size, following recommendations from previous validation studies (Gexcon, 2015).

For the configurations with a vent opening of 5.4 m^2, pressure reflections from the Euler boundary condition artificially enhances the second pressure peak, as observed by Vyazmina & Jallais (2015). To reduce this effect, all boundary conditions were therefore set to type “plane wave”, a version of the Euler boundary conditions with non-reflective properties. For this setting, selected scenarios were run with an increased simulation domain of size 120 m × 120 m × 60 m. Fig. 3 (right) shows the corresponding results for centre ignition and a 5.4 m^2 vent opening, plotted together with results obtained by using the standard domain size of 40 m × 30 m × 12 m. The boundary effects in Fig. 3 (right) are considered negligible.

4.1.4 Model representation of physical phenomena

This section presents a few selected pressure-time and flame speed curves for tests with 18 vol % hydrogen, initial u' of 0.1 m/s, with back, centre or front ignition, and vent sizes of 5.4 m^2 or 2.7 m^2 (Bauwens *et al.*, 2011). Section 4.1.6 offers some discussion and analysis of the results.

The settings indicated in sections 4.1.1-4.1.3 were used for all simulations. A 80 Hz low-pass filter had been applied to the experimental pressure-time curves extracted from (Bauwens *et al.*, 2011).

Fig. 4 (left) shows the pressure-time curves for back ignition, with a 5.4 m^2 vent opening. Fig. 4 (right) shows the corresponding flame speed vs. distance from ignition. The grey vertical lines in Fig. 4 mark the simulated flame arrival at the vent opening (left), and the position of the vent (right). FLACS v10.4r2 over-predicts the initial flame speed (up to 3 m from ignition) by 20-50 %, leading to an earlier and more significant pressure-rise than in the experiments. As the flame front approaches and passes through the vent opening, the model persists in over-predicting the flame speed. As observed in the experiment, the simulated pressure-rise decreases for a short period of time right after flame arrival at the vent opening, as low-density combustion products are vented from the chamber. Similar to the experiment, FLACS v10.4r2 subsequently produces a distinct pressure peak generated by the external explosion (occurring 200 ms after ignition, after the exit of the flame front through the vent). Following the external explosion, the Helmholtz-oscillations observed in the experiment are under-predicted by the model.

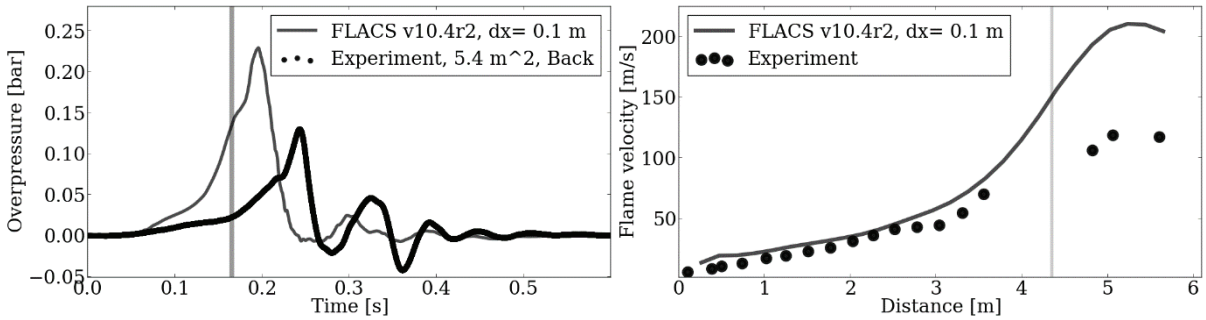

Fig. 4 *Pressure-time (left), and flame speed vs. distance from ignition point (right), back ignition, 5.4 m^2 vent. The grey vertical lines mark the simulated flame arrival at the vent opening (left), and the position of the vent (right).*

Fig. 5 shows the pressure-time curves for front ignition, with a 2.7 m^2 vent opening (left), and a 5.4 m^2 vent opening (right). FLACS v10.4r2 closely matches the experimental results up to 150 ms after ignition for both configurations. However, from 200 ms after ignition, the model starts predicting a more significant pressure-rise than observed in the experiments, producing a pressure peak right before the flame front reaches the chamber walls. These results are consistent with the results observed in Fig. 4; FLACS v10.4r2 consistently over-estimates the experimental flame speed throughout the explosion history. FLACS-Hydrogen cannot reproduce the coupling that develops between acoustics in the chamber and the structure, and the subsequent enhancement of the flame surface, as appropriate sub-grid models currently are not implemented (cf. Section 3.1.1). Therefore, the model does not reproduce P_{vib}, the main pressure peak occurring at approximately 600 ms in the front ignition experiments.

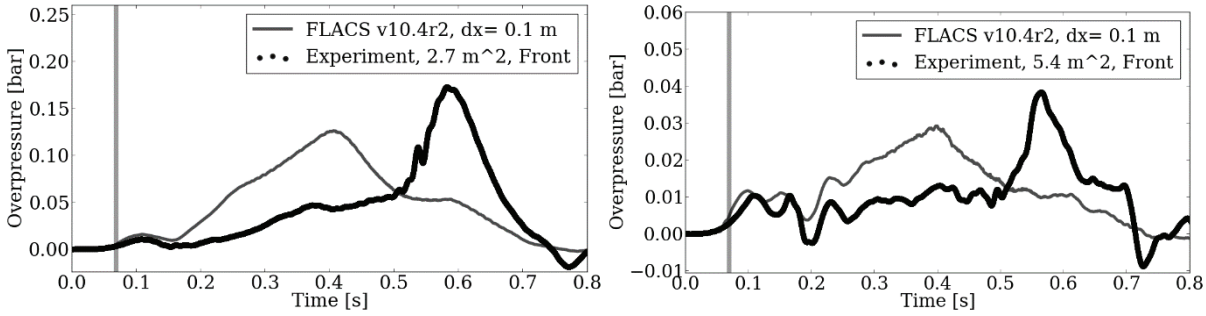

Fig. 5 *Pressure-time, front ignition, 2.7 m^2 vent (left) and 5.4 m^2 vent (right).*

Fig. 6 (left) shows the pressure-time curves for back ignition, with a 2.7 m^2 vent opening. Consistently with the previous results for 18 % hydrogen mixtures, FLACS v10.4r2 over-predicts the pressure-rise in the initial phase of flame propagation, prior to the flame arrival at the vent opening. The simulated maximum overpressure peak occurs as the flame front reaches the chamber walls. Fig. 6 (right) shows the pressure-time curves for centre ignition, with a 5.4 m^2 vent opening. FLACS-Hydrogen predicts two distinct separate pressure peaks for this configuration; the first peak is due to the external explosion, while the second peak is produced as the flame reaches the chamber walls, and the maximum flame surface area inside the chamber is obtained. FLACS v10.4r2 significantly over-predicts the overpressure from the external explosion. Low-frequency pressure oscillations (approximately 100 Hz) can be discerned in the simulations between 200 and 300 ms, generated as the flame surface approaches the chamber walls. The low-frequency oscillations match the first fundamental mode of a wave propagating inside the chamber parallel to the vent opening, assuming the chamber is filled with combustion products (Bauwens *et al.*, 2009). These oscillations are also present, although barely noticeable, in the pressure-time curves for all configurations, e.g. after the external explosion peak in Fig. 4. Note that the second pressure peak in Fig. 6 (right) is not generated by artificial reflections from the simulation boundaries (cf. Section 4.1.3 and Fig. 4, right).

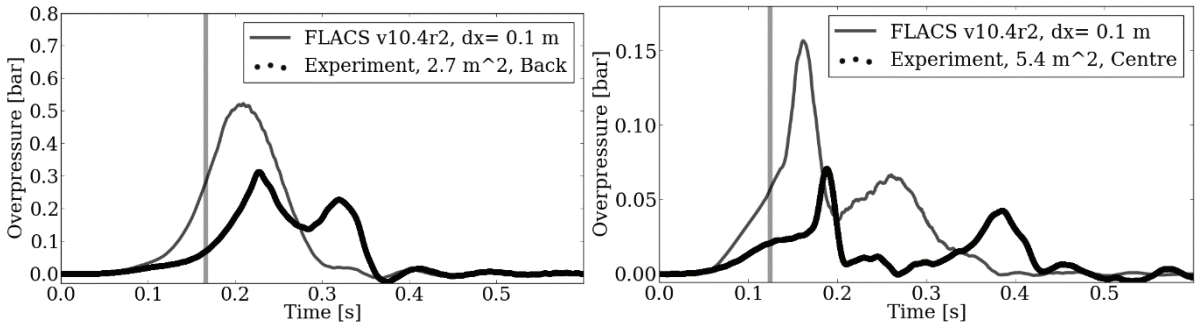

Fig. 6 *Pressure-time, back ignition, 2.7 m^2 vent (left) and centre ignition, 5.4 m^2 vent (right).*

4.1.5 Quantitative assessment and visualisation of results

Fig. 7 (left) shows a *scatter plot* of the primary validation target P_{ext} for all the relevant tests from (Bauwens *et al.*, 2011; Chao *et al.*, 2011; Bauwens *et al.*, 2012; Bauwens & Dorofeev, 2014) involving an empty enclosure. This type of graphical representation represents a quick and straightforward way of comparing results from experiments and simulations. The diagonal ($y = x$) represents perfect agreement, points above the diagonal represent over-prediction, and points below the diagonal represent under-prediction. As a minimum, FAC2 should be visualised in the scatter plots, however, stricter bounds may also be applied to the data set.

Fig. 7 (right) shows a *parabola plot* of the complete data set from Fig. 7 (left), i.e. a graphical presentation where the geometric mean bias (MG) for the data set is plotted against the corresponding geometric mean variance (VG) (cf. Table 7). The parabola represents the curve of zero arithmetic variance, the line $x = 1$ represents unbiased results; perfect agreement is therefore represented by the point (1,1). The experimental variability for P_{ext} is plotted in Fig. 7 (right) together with the zero-variance parabola. The presentation of the results should reflect the model performance under the various initial and geometric conditions affecting the governing physical phenomena, to identify overall trends for the different configurations. In Fig. 7 (right), MG and VG for tests with centre and back ignition are plotted separately, the same is done for tests performed with a hydrogen concentration higher or lower than 17.5 %. The criteria for “excellent” and “acceptable” model performance in terms of VG and MG are also visualised in Fig. 7 (right).

When considering the results from all campaigns with lean hydrogen-air mixtures in empty enclosures from (Bauwens *et al.*, 2011; Chao *et al.*, 2011; Bauwens *et al.*, 2012; Bauwens & Dorofeev, 2014) together, the model performance is within the “acceptable” criteria, with MG = 1.83, VG = 1.67, and FAC2 = 58 %. However, when considering centre and back ignition tests separately, the bias towards over-prediction for centre ignition in terms of MG is 2.16, which is slightly higher than the criterion MG ≤ 2. Furthermore, for centre ignition, FAC2 = 36 %, i.e. below the “acceptable” criterion of 50 %. Meanwhile, the back ignition tests are well within the currently defined criteria for “acceptable” model performance. Fig. 7 (right) also shows that P_{ext} for mixtures with more than 17.5 % hydrogen is over-predicted compared to the leaner mixtures, with MG = 2.14 and FAC2 = 43 %. These results warrant further investigation, cf. Section 4.1.6.

4.1.6 Discussion: results and possible model improvements

Fig. 7 shows that FLACS v10.4r2 generally gives conservative results for the maximum overpressure due to the external explosion, P_{ext}, for fuel-lean hydrogen-air deflagrations in empty vented enclosures. The results are particularly conservative for centre ignition. FLACS v10.4r2 is seen to over-predict the flame speed for mixtures with a hydrogen concentration exceeding 17.5 % almost from the time of ignition. In the simulations, the quasi-laminar regime

governs the flame acceleration prior to the exit of the flame through the vent, while turbulent combustion mainly occurs externally to the chamber. The Lewis-number corrected laminar burning velocity (cf. Section 3.1.1) is likely over-predicted at the present fuel concentrations. Implementing updated Markstein number dependent burning velocity correlations for both quasi-laminar and turbulent combustion (Hisken *et al.*, 2015) will likely improve these results.

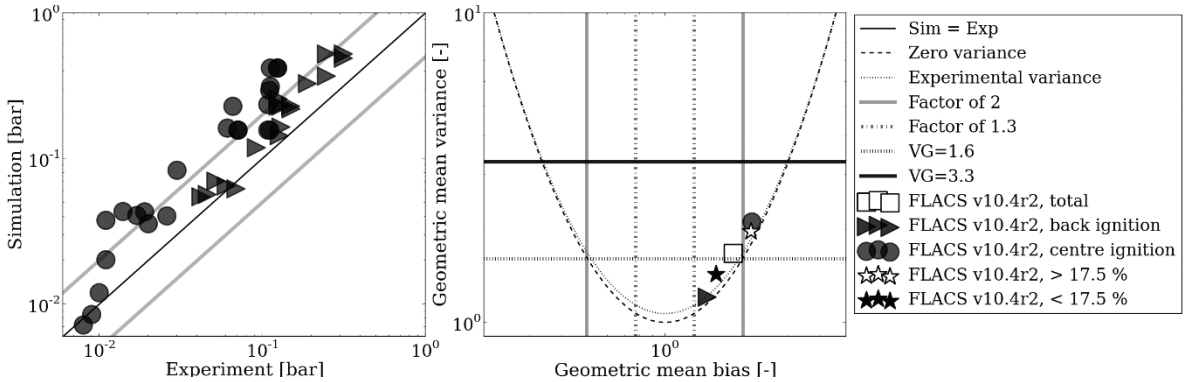

Fig. 7 *Scatter plot (left) and parabola plot (right) of the pressure peak* P_{ext}, *for all campaigns in the present study.*

For FLACS v10.4r2, using the *k-ε* turbulence model, the primary external explosion seems to be sufficiently represented by turbulence production alone for the present flame speeds. Strictly, accurate representation of the external explosion may require that Rayleigh-Taylor instability effects are explicitly accounted for in the combustion model. Including this effect may also improve the representation of the Helmholtz oscillations in the configurations with back ignition and a 5.4 m^2 vent opening observed in Fig. 4 (left). Furthermore, the amount of unburnt mixture in the chamber in the simulations at the onset of the oscillations is likely less than in the experiments, which may also contribute to the under-prediction of Helmholtz oscillations.

The front ignition experiments (cf. Fig. 5) demonstrated that the pressure peak P_{vib} cannot be represented by FLACS-Hydrogen, as the model lacks sub-grid models accounting for flame-acoustic interactions. For centre ignition and a vent opening of 5.4 m^2, FLACS v10.4r2 still reproduces a second distinct pressure peak in addition to P_{ext} occurring at the time when the maximum simulated flame area inside the chamber is obtained. With a 2.7 m^2 vent opening, this simulated second pressure peak is merged together with P_{ext}, and likely contributes to the over-prediction of the centre ignition overpressures relative to back ignition observed in Fig. 7.

5. Conclusions

Developing consequence prediction tools for hydrogen safety applications requires a validation methodology that systematically evaluates the tool's ability to reproduce relevant physical phenomena. In order to define the application range of the tool, model evaluation should be performed according to an established model evaluation protocol (MEP). The present paper demonstrated how a MEP, based on recent developments in the community of hydrogen safety, can be applied specifically for consequence assessment of accidental explosion scenarios involving hydrogen mixtures in vented small-scale enclosures or 20 ft./40 ft. ISO containers. As an example, the present study outlined the evaluation of FLACS-Hydrogen, version 10.4, release 2, for an experimental campaign involving hydrogen deflagrations in empty vented enclosures. It is straightforward to extend the present study with additional experiments from the validation database. The present approach was found to be highly useful for identifying areas of satisfactory model performance as well as limitations, and will provide a useful tool in the continued model development.

Acknowledgements

The research leading to these results is part of a project that has received funding from the Fuel Cells and Hydrogen 2 Joint Undertaking under grant agreement No. 671461. This Joint Undertaking receives support from the European Union's Horizon 2020 research and innovation programme and United Kingdom, Italy, Belgium and Norway.

References

Abdel-Gayed R.G., Bradley D., Lawes M. (1987). Turbulent burning velocities: A general correlation in terms of straining rates, Proc. R. Soc. Lond. A, 414, 389–413.

Arntzen, B.J. (1998). Modelling of turbulence and combustion for simulation of gas explosions in complex geometries. Dr. Ing. Thesis, NTNU, Trondheim.

Baraldi, D., Kotchourko, A., Lelyakin, A., Yanez, J., Gavrikov, A., Efimenko, A., Verbecke, F., Makarov, D., Molkov, V. & Teodorczyk, A. (2010). An inter-comparison exercise on CFD model capabilities to simulate hydrogen deflagrations with pressure relief vents. International Journal of Hydrogen Energy. 35(22): 12381-12390.

Baraldi, D., Melideo, D., Kotchourko, A., Ren, K., Yanex, J., Jedicke O., Giannissi, S.G., Tolias, I.C., Venetsanos, A.G., Keenan, J., Makarov, D., Molkov, V., Slater, S., Verbecke, F. & Duclos, A. (2015). Development of a model evaluation protocol for CFD analysis of hydrogen safety issues – the SUSANA project. Sixth International Conference on Hydrogen Safety (ICHS), Yokohama, 19-21 October 2015: 15 pp.

Barenblatt, G.I., Zel'dovich, Ya. B. & Istratov, A.G. (1962). On the diffusive-thermal stability of a laminar flame. Journal of Applied Mech. Tech. Phys. 4: 21-26.

Bauwens, C.R., Chaffee, J. & Dorofeev, S. (2009). Effect of instabilities and acoustics on pressure generated in vented propane-air explosions. Twenty-second International Colloquium on Dynamics of Explosions and Reactive Systems (ICDERS), 27-31 July, Minsk, Belarus: 4 pp.

Bauwens, C.R., Chaffee, J. & Dorofeev, S.B. (2011). Vented explosion overpressures from combustion of hydrogen and hydrocarbon mixtures. International Journal of Hydrogen Energy, 36(3): 2329-2336.

Bauwens, C.R., Chao, J. & Dorofeev, S.B. (2012). Effect of hydrogen concentration on vented explosion overpressures from lean hydrogen–air deflagrations. International Journal of Hydrogen Energy, 37(22): 17599-17605.

Bauwens, C.R. & Dorofeev, S.B. (2014). Effect of initial turbulence on vented explosion overpressures from lean hydrogen–air deflagrations. International Journal of Hydrogen Energy, 39(35): 20447-20454.

Bradley, D., Gaskell, P., Gu, X. & Sedaghat, A. (2005). Premixed flamelet modelling: factors influencing the turbulent heat release rate source term and the turbulent burning velocity. Combustion and Flame, 143(3): 227–245.

Bradley, D., Lawes, M., Liu, K. & Mansour, M. (2013). Measurements and correlations of turbulent burning velocities over wide ranges of fuels and elevated pressures. Proceedings of the Combustion Institute, 34(1): 1519 – 1526.

Bray K.N.C. (1990). Studies of the turbulent burning velocity, Proc. R. Soc. Lond. A, 431, 315–335.

Chao, J., Bauwens, C. & Dorofeev, S. (2011). An analysis of peak overpressures in vented gaseous explosions. Proceedings of the Combustion Institute, 33(2): 2367-2374.

Cooper, M.G., Fairweather, M. & Tite, J.P. (1986). On the mechanisms of pressure generation in vented explosions. Combustion and flame, 65: 1-14.

Darrieus, G. (1938). Propagation d'un front de flamme. Presented at La Technique Moderne (Paris) and in 1945 at Congrès de Méchanique Appliquée (Paris).

Daubech, J., Proust, C., Jamois, D. & Leprette, E. (2011). Dynamics of vented hydrogen-air deflagrations, Proceedings of 4th ICHS, September 2011, San Francisco.

Daubech, J., Proust, Ch., Gentilhomme, O., Jamois, D. & Mathieu, L. (2013). Hydrogen-air vented explosions: new experimental data. Proceedings of 5th ICHS, September 2013, Brussels.

Duijm, N.J., & Carissimo, B. (2002). Evaluation methodologies for dense gas dispersion models. In M. Fingas (Ed.): the handbook of hazardous materials spills technology, McGraw-Hill: pp. 19.1-19.22.

Gexcon AS. (2015). FLACS v10.4r2 User's Manual. Confidential report. Gexcon AS, Bergen, Norway.
Groth, K.M. & Hecht, E.S. (2015). HyRAM: A methodology and toolkit for quantitative risk assessment of hydrogen systems. Sixth International Conference on Hydrogen Safety, 19-21 October 2015, 11 pp.
Hanna, S.R., Strimaitis, D.G. & Chang, J.C. (1991a). Hazard response modelling uncertainty (a quantitative method) – Vol. I: User's guide for software for evaluating hazardous gas dispersion models. Sigma Research Corporation, Westford, USA.
Hanna, S.R., Strimaitis, D.G. & Chang, J.C. (1991b). Hazard response modelling uncertainty (a quantitative method) – Vol. II: Evaluation of commonly-used hazardous gas dispersion models. Sigma Research Corporation, Westford, USA.
Hanna, S.R., Chang, J.C. & Strimaitis, D.G. (1993). Hazardous gas model evaluation with field observations. Atmospheric Environment, 27A: 2265-2285.
Hisken, H., Enstad, G.A., Middha, P. & van Wingerden, K. (2015). Investigation of concentration effects on the flame acceleration in vented channels. Journal of Loss Prevention in the Process Industries, 36: 447-459.
Hjertager, B.H. (1986). Three-dimensional modeling of flow, heat transfer, and combustion. In Handbook of Heat and Mass Transfer, Gulf Publishing, Houston, Chapter 41: 1303-1350.
Ivings, M.J., Jagger, S.F., Lea, C.J. & Webber, D.M. (2007). Evaluating vapour dispersion models for safety analysis of LNG facilities. Fire Protection Research Foundation, National Fire Protection Association. http://www.nfpa.org/assets/files/PDF/Research/LNGVaporDispersionModel.pdf. Accessed 20.02.2016.
Ivings, M. J., Lea, C. J., Webber D. M., Jagger, S. F. & Coldrick, S. (2013). A protocol for the evaluation of LNG vapour dispersion models, Journal of Loss Prevention in the Process Industries, 26: 153-163.
Jallais, S. & Kudriakov, S. (2013). An inter-comparison exercise on engineering models capabilities to simulate hydrogen vented explosions. Proceedings of 5th ICHS, September 2013, Brussels: 13 pp.
Landau, L.D. (1944). On the theory of slow combustion. Zh. Eksp. i Theor. Fiz. 14, 240.
Launder B.E. & Spalding D.P. (1974) The numerical computation of turbulent flows. Comput. Meth. Appl. Mech. Eng., 3(2): 269-289.
Keenan, J.J., Makarov, D.V. & Molkov, V.V. (2014). Rayleigh–Taylor instability: Modelling and effect on coherent deflagrations. International Journal of Hydrogen Energy, 39(35): 20467-20473.
Kumar, R.K. (2006). Vented combustion of hydrogen-air mixtures in a large rectangular volume. Collection of technical papers - 44th AIAA Aerospace Sciences Meeting, 6: 4398-4406.
Kuznetsov, M., Friedrich, A., Stern, G., Kotchourko, N., Jallais, S. & L'Hostis, B. (2015). Medium-scale experiments on vented hydrogen deflagration. Journal of Loss Prevention in the Process Industries, 36: 416 – 428.
Makarov, D. & Molkov, V. (2013). Numerical simulation of 10% hydrogen-air vented deflagration in a 120 m^3 enclosure. Proceedings Seventh International Seminar on Fire and Explosion Hazards (ISFEH), Providence, 5-10 May 2013, published by Research Publishing, Singapore: 975–984. ISBN: 978-981-07-5936-0.
Marangon, A., Schiavetti, M., Carcassi, M., Pittiglio, P., Bragatto, P. & Castellano, A. (2009). Turbulent hydrogen deflagration induced by obstacles in real confined environment. International Journal of Hydrogen Energy, 34(10): 4669–4674.
Middha, P. (2010). Development, use, and validation of the CFD tool FLACS for hydrogen safety studies. PhD thesis, Department of Physics and Technology, University of Bergen.
Model Evaluation Group (MEG). (1994a). Model evaluation protocol. Model Evaluation Group, European Communities, Directorate-General XII, Science Research and Development, May 1994.
Model Evaluation Group (MEG). (1994b). Guidelines for model developers. Model Evaluation Group, European Communities, Directorate-General XII, Science Research and Development, May 1994.
Model Evaluation Group Gas Explosions (MEGGE). (1996). Gas Explosion Model Evaluation Protocole, Version 1, Technical Report.
Pasman, H.J., Groothuisen, T. M. & Gooijer, P.H. (1974). Design of pressure relief vents. In: Buschman C.H., editor: Loss Prevention and Safety Promotion in the Process Industries. New-York: Elsevier: 185–189.

Patankar, S.V. & Spalding, D.B. (1974). A calculation procedure for the transient and steady-state behaviour of shell-and-tube heat exchangers. Heat Exchangers: Design and Theory Sourcebook, McGraw-Hill, pp. 155–176.

Ranzi, E., Frassoldati, A., Grana, R., Cuoci, A., Faravelli, T., Kelley, A. & Law, C. (2012). Hierarchical and comparative kinetic modeling of laminar flame speeds of hydrocarbon and oxygenated fuels. Progress in Energy and Combustion Science, 38(4):468–501.

Schiavetti, M. & Carcassi, M. (2013). UNIPI activities with FLACS code. Report 2012-2013, University di Pisa.

Sha, W.T. & Launder, B.E. (1979). A model for turbulent momentum and heat transport in large rod bundles. Report ANL-77-73. Illinois: Argonne National Laboratory.

Sha, W.T., Yang, C.I., Kao, T.T. & Cho, S.M. (1982). Multidimensional numerical modeling of heat exchangers. Journal of Heat Transfer, 104(3): 417–425.

Sivashinsky, G. (1977). Diffusional-thermal theory of cellular flames. Combustion Science and Technology, 15 (3-4): 137–145.

Skjold, T., Pedersen, H.H., Bernard, L., Ichard, M., Middha, P., Narasimhamurthy, V.D., Landvik, T., Lea, T & Pesch, L. (2013). A matter of life and death: validating, qualifying and documenting models for simulating flow-related accident scenarios in the process industry, Chemical Engineering Transactions, 31: 187–192.

Skjold, T., Groth, K.M., LaFleur, A.C., Siccama, D., Middha, P., Hisken, H. & Brambilla, A. (2015). 3D Risk management for hydrogen installations (Hy3DRM). Sixth International Conference on Hydrogen Safety (ICHS), Tokyo, Japan, 19-21 October 2015: 11 pp.

Sommersel, O.K., Bjerketvedt, D., Christensen, S., Krest, O. & Vaagsaether, K. (2008). Application of background oriented schlieren for quantitative measurements of shock waves from explosions. Shock Waves, 18(4): 291–297.

Sommersel, O.K., Vaagsather, K. & Bjerketvedt, D. (2015). Hydrogen explosions in 20’ container. Sixth International Conference on Hydrogen Safety (ICHS), Tokyo, Japan, 19-21 October 2015: 12 pp.

Vyazmina, E. & Jallais, S. (2015). Validation and recommendations for CFD and engineering modelling of hydrogen vented explosions: Effects of concentration, obstruction and vent area. International Conference on Hydrogen Safety (ICHS), Yokohama, 19-21 October 2015: 10 pp.